18th Australasian Fluid Mechanics Conference
Launceston, Australia
3-7 December 2012

Measurements of streamwise and spanwise fluctuating velocity components in a high Reynolds number turbulent boundary layer

R. Baidya, J. Philip, N. Hutchins, J. P. Monty and I. Marusic

Department of Mechanical Engineering
The University of Melbourne, Victoria, 3010 AUSTRALIA

Abstract

Measurements of the streamwise and spanwise fluctuating velocity components are obtained in a high Reynolds number turbulent boundary layer using custom made sub-miniature hot wires. These measurements are made over a range of Reynolds numbers from $Re_\tau \approx 3,000$ to $Re_\tau \approx 10,500$, but at fixed unit Reynolds number U_∞/ν ($Re_\tau = \delta U_\tau/\nu$; where ν is the kinematic viscosity, U_τ is the friction velocity and δ is the boundary layer thickness). In this way the measurement volumes of the probes are approximately fixed for all Re_τ at $14\times14\times7$ viscous units. This gives sufficiently resolved velocity measurements, allowing observation of Re_τ trends in isolation from spatial resolution effects.

The resulting velocity measurements show clear scale separation in both streamwise and spanwise velocities at $Re_\tau \approx 10,500$. The pre-multiplied spectra for both components show a near-wall peak which is fixed in viscous units and an outer region peak fixed in outer scaling, which grows in magnitude with Re_τ. The large scale wavelengths associated with the outer site extend all the way down to the near-wall region for both components demonstrating the presence of large scale motions with a footprint that stretches to the surface for both of the streamwise and spanwise fluctuations.

Introduction

The broad-band nature of turbulence, and the increased scale separation between the smallest and largest energetic scales as Reynolds number increases, mean that it is highly challenging to obtain well resolved measurements of fluctuating components in high Reynolds number flows. Hot-wire anemometry using a single-wire has been successfully applied to obtain sufficiently resolved streamwise velocity components at a high Re [4]; however, there is a dearth of measurements for the other two velocity components at similarly high Re. Here, we attempt to redress this issue by simultaneously measuring the streamwise and spanwise fluctuating velocity components using sub-miniature cross-wires.

For this paper, we highlight the similarities and the differences in Reynolds number trends for the streamwise and spanwise components. We consider in particular, the contribution from small and large scales in the flow to the turbulence intensities and the pre-multiplied spectra. Here, we use superscript '+' to denote viscous scaling of length (e.g. $z^+ = zU\tau/\nu$), velocity (e.g. $U^+ = U/U\tau$) and time (e.g. $t^+ = tU_\tau^2/\nu$). Capitalisation (e.g. U) and overbar (e.g. $\overline{u^2}$) indicate time averaged quantities, while lower case (e.g. u) shows fluctuating components. We employ the co-ordinate system x, y and z to refer to streamwise, spanwise and wall-normal directions; with u, v and w the corresponding fluctuating velocities.

Apparatus

Facility

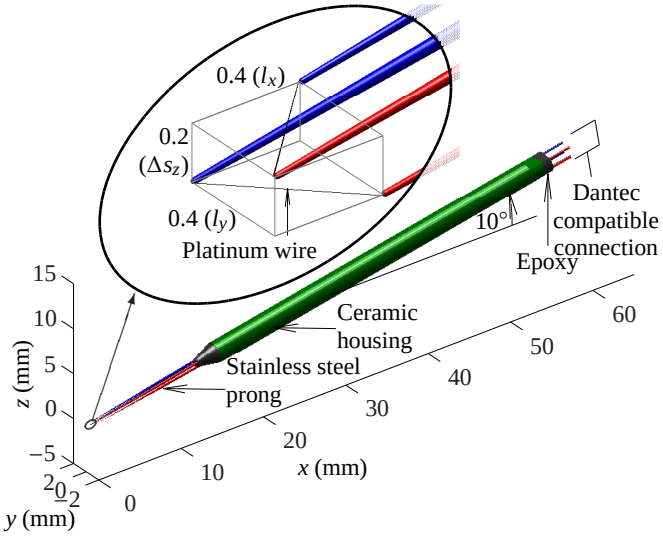

Figure 1: (main figure) Custom cross-wire probe, (inset figure) expanded view of the prong tips, with cuboid volume of $0.4\times0.4\times0.2$mm shown overlaid. All dimensions in mm.

The experiments are conducted in the High Reynolds Number Boundary Layer Wind Tunnel (HRNBLWT), located at the University of Melbourne. This is an open-return blower tunnel with a working section of $27\times2\times1$m with a boundary layer thickness of up to 0.35m. This facility follows the 'big and slow' approach, meaning that high Reynolds numbers are attained in boundary layers where the smallest length and time scales are still accessible to conventional measurement techniques. For example at $Re_\tau \approx 10,000$, the viscous length scale is approximately 30μm and viscous time scale is approximately 60μs. This permits the use of 2.5μm diameter (d) hot-wires which are in general less prone to breakages and drift than the smaller diameter wires ($d \leq 1.5$μm) while maintaining viscous scaled sensor length of approximately 20 ($l^+ \approx 20$), and thus providing sufficiently resolved velocity measurements.

Probes

All the cross-wire probes are custom made in the laboratory. This has been primarily driven by the lack of a commercially available cross-wire probe smaller than $1.2\times1.2\times1.2$mm. Also, with the commercially available probes, the closest wall-position attainable with sensing elements parallel to the wall is 3mm when accounting for the probe holder. This corresponds to $z^+ \approx 100$ at the Reynolds number of these experiments, rendering the entire buffer zone inaccessible. For our custom cross-wire probe, we settled on a final dimension of 0.4×0.4mm in the streamwise and spanwise direction with a wall-normal spacing of 0.2mm. To allow access close to the wall and minimise blockage effects, the probe has been manufactured such that the sensing elements are parallel to the wall when the probe is inclined at 10° to the horizontal. Figure 1 (main) shows

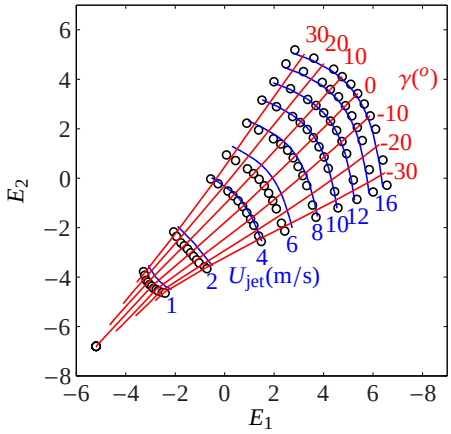

Figure 2: Typical jet calibration showing calibration points (○), constant jet velocity lines (—) and constant yaw angle lines (—) determined from calibration points.

the custom probe, which is constructed from four 250μm diameter stainless steel prongs and a ceramic body held together by epoxy resins. The prong tips are sharpened using a grinding process so that the tip diameter tapers down to 20μm over 10mm. The platinum wires are then welded across the prong tips, as shown in expanded view in figure 1. For clarity, the prongs closest to the viewer have been coloured red in figure 1 (those furthest away are coloured blue). Figure 1 (inset) also shows a cuboidal volume with dimensions of $0.4\times0.4\times0.2$mm ($l_x\times l_y\times\Delta s_z$) encapsulating the sensing elements. The back end of the custom probe is designed to be compatible with the standard Dantec cross-wire probe holders (55H25).

Calibration

The calibration is performed *in situ* to eliminate the need for the probe to be moved between the calibration and measurement stage. This removes the possibility of probe misalignment between the calibraton and the measurement, improving the overall accuracy of the experiments. The calibration facility consists of a jet mounted on a two-axis-traverse allowing rotation with two degrees of freedom. For the calibration of the wires measuring streamwise and spanwise velocities, the probe is placed at the axis of the rotation and the jet is yawed using a stepper motor about wall-normal axis. An encoder attached to the axis provides an accurate measurement of angle of the jet relative to the wire. For different jet velocities (U_{jet}) and calibration yaw angles (γ), the corresponding voltages from wire 1 and 2 (E_1 and E_2) are recorded to build a voltage to velocity conversion map. A typical calibration curve is shown in figure 2. Blue and red lines show contours of constant U_{jet} and γ respectively, determined from the calibration data using linear interpolation.

Results

Experiments have been conducted using the custom cross-wire to measure u and v simultaneously at various streamwise locations ($2 < x < 18$m) from the trip while matching the unit Reynolds number (U_∞/ν, where U_∞ is the free-stream velocity). In this manner the same probe geometry affords approximately matched viscous-scaled sensor length (l^+) and sensor spacing (Δs^+) (since U_τ variation in x is very small, l^+ or Δs^+ variation is limited to ±1 viscous unit) across the entire range of Re_τ. This aids in observing the Re_τ trends relatively free of spatial resolution effects [2]. Consequently, the probes have matched measurement volumes of approximately $14\times14\times7$ (±10%) viscous length scales across all Re_τ. The

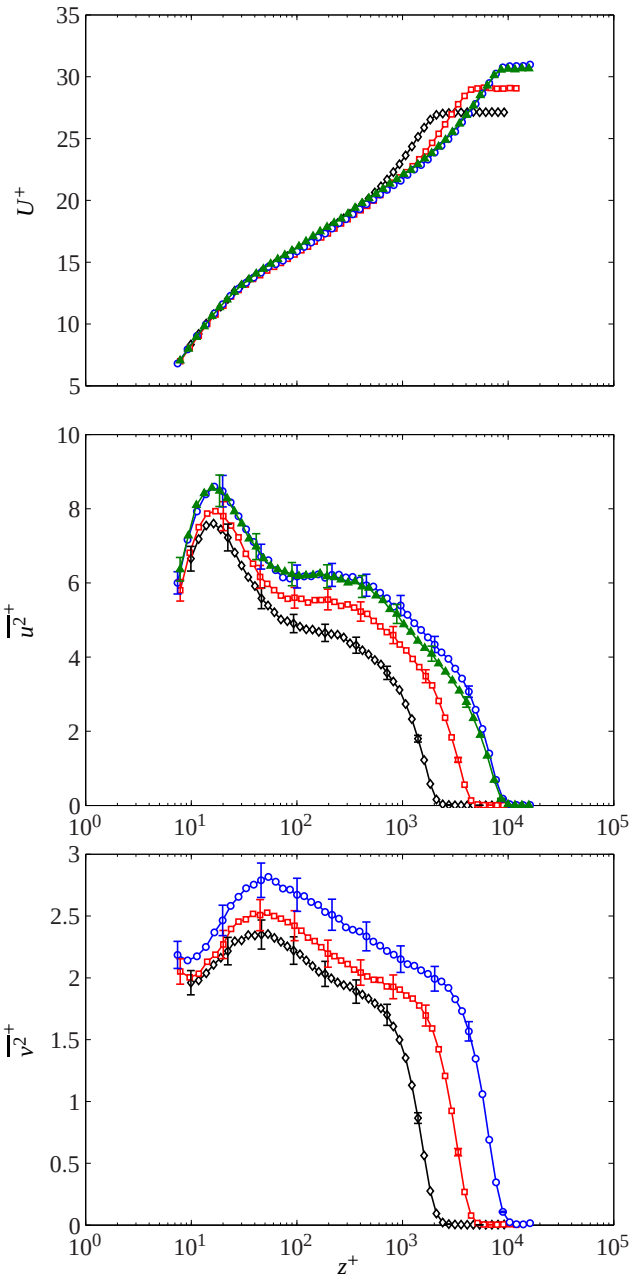

Figure 3: Mean (top), streamwise turbulence intensity (middle) and spanwise turbulence intensity (bottom) as functions of wall-normal positions (z^+) for various Reynolds numbers (Re_τ); ▲ - $Re_\tau \approx 10{,}500$, ○ - $Re_\tau \approx 10{,}500$, □ - $Re_\tau \approx 6{,}000$, ◊ - $Re_\tau \approx 3{,}000$; solid symbol - single-wire; open symbol - cross-wire; vertical bars on the turbulence intensities profile are the associated repeatability of the measurement.

friction velocity U_τ is determined from the mean velocity profile using a Rotta-Clauser fit [5].

Statistics

The streamwise mean velocity profiles and turbulence statistics from the cross-wire are shown in figure 3 with open symbols for three different Re_τ. A single wire measurement with matched U_∞/ν and l^+ at $Re_\tau \approx 10{,}500$ is also shown with solid symbols. It can be seen that both the streamwise mean and turbulence intensity measurements from the cross-wire agree well with the single-wire results and any discrepancy is within the experimen-

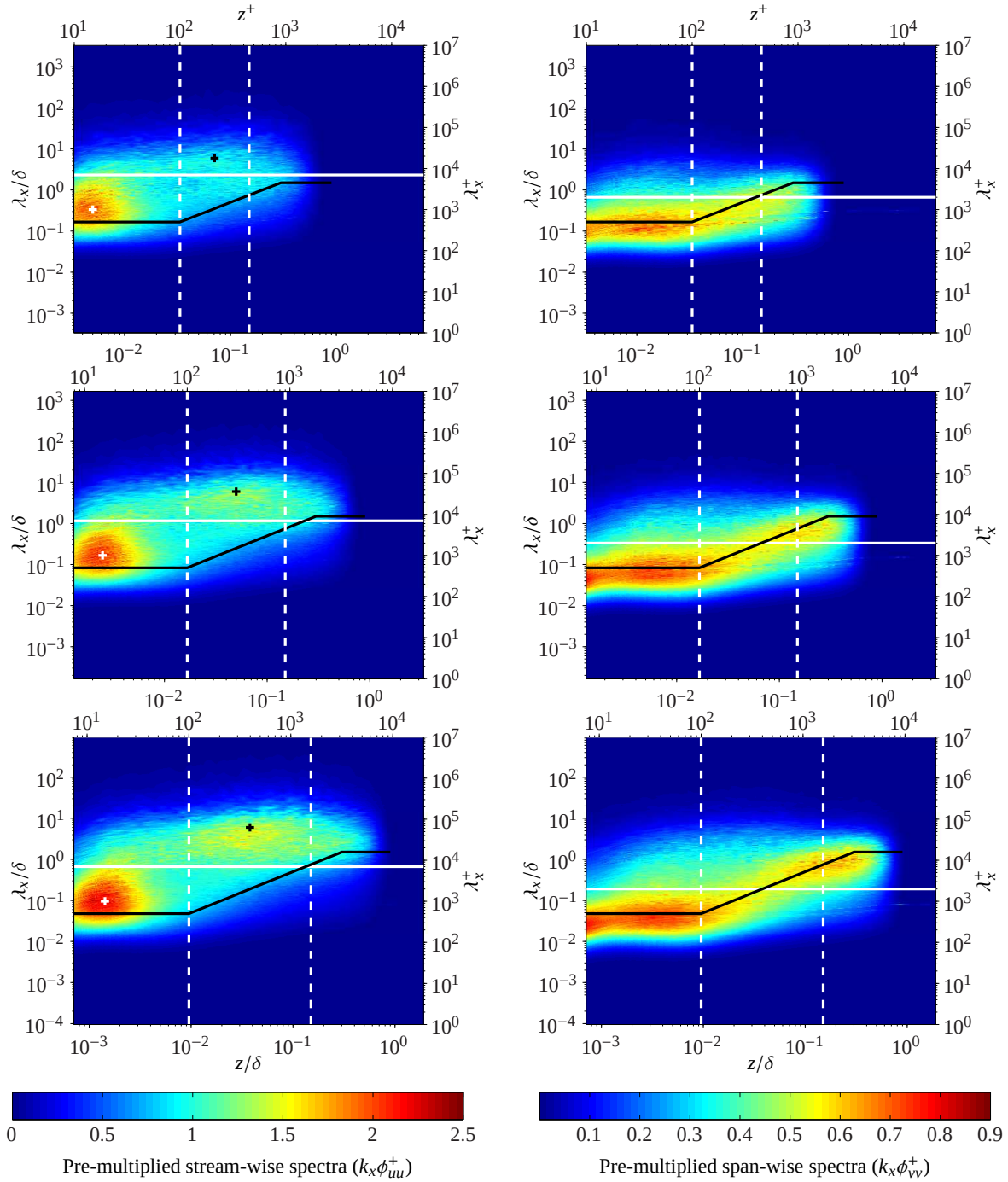

Figure 4: Two dimensional pre-multiplied spectra at $Re_\tau \approx 3{,}000$ (top), 6,000 (middle) and 10,500 (bottom); horizontal white line indicate cutoff wave length between small and large scale for each pre-multiplied spectra; dashed white vertical lines indicate location $z^+ = 100$, $0.15\delta^+$; '+' symbols show location of inner (white) and outer (black) energy sites for $k_x\phi_{uu}^+$; black line shown is $\lambda_x^+ = 500$ ($z^+ < 100$), $\lambda_x^+ = 5z^+$ ($100 < z^+ < 0.3\delta^+$), $\lambda_x^+ = 1.5\delta^+$ ($z^+ > 0.3\delta^+$).

tal errors. The errors associated with the mean measurements are indicated by the size of the symbols ($\pm 0.01U^+$ [3]), while the repeatability of measurements associated with the turbulent intensity measurements are indicated by vertical bars ($\pm 0.04\overline{u^2}$ and $\pm 0.04\overline{v^2}$ for streamwise and spanwise, respectively). The peak spanwise turbulence intensity occurs at $z^+ \approx 50$ which is further away from the wall than the streamwise intensity peak location at $z^+ \approx 15$. The measurements suggest that both the streamwise and spanwise turbulence intensities grow with the Reynolds number, as the difference between intensities for the smallest and largest Re_τ is several times greater than the expected errors. Both spanwise and streamwise turbulence intensities, are also seen to exhibit a logarithmic region in support of the attached eddy hypothesis of Townsend [6]. These features are the subject of further investigation.

Pre-multiplied spectra

Figure 4 shows pre-multiplied spectra maps for both the streamwise and spanwise velocity fluctuations for the three Reynolds number $Re_\tau \approx 3{,}000$, $6{,}000$ and $10{,}500$. The energy spectra

for the streamwise fluctuations (left-hand plots) follow similar trends to those observed by Hutchins *et al.* [1]. An inner energetic peak associated with the near-wall cycle remains approximately fixed at $z^+ \approx 15$ and $\lambda_x^+ \approx 1000$. However, as Reynolds number increases, a large-scale energetic peak emerges in the log region approximately located at $z^+ \approx \sqrt{15 Re_\tau}$ and $\lambda_x^+ \approx 6\delta$. The inner and outer energetic sites are marked by the white and black '+' symbols respectively. As Reynolds number increases, the symbols become increasingly separated in z^+ and λ_x^+ reflecting the increasing scale separation.

The energy spectra for the spanwise fluctuations (right-hand plots) are very different. There are no clear inner or outer energetic peaks in the sense of the u spectra. Rather it appears that for $z^+ < 100$, there is a clear ridge of energy at $\lambda_x^+ \approx 500$. Through the log region there are clear signs of energy scaling with distance from the wall, with the energetic ridge seeming to follow $\lambda_x^+ = 5z^+$ for $100 < z^+ \lesssim 0.3\delta^+$. For the wake region the energy seems to reach a ridge at constant $\lambda_x/\delta = O(1)$. The energetic ridge in v spectra is indicated by the black lines in figure 4. It is evident that the bulk of the energy in the streamwise fluctuations is confined to a larger wavelengths than the line representing the energetic ridge in v spectra. Hence, this line seems to correspond to a demarcation between non-energetic and energetic wavelengths in u spectra for $z^+ > 100$.

Scale separation

Figure 5 shows contributions to turbulence intensities from the small and large scales as a function of wall-normal distance. The cut-off wavelength between the small and large scales for steamwise and spanwise is at $\lambda_x^+ \approx 7{,}000$ and $\lambda_x^+ \approx 2{,}000$, respectively; and are shown as horizontal white lines in figure 4. As expected, the small scale contributions collapse for both streamwise and spanwise velocities for $z^+ < 100$, while the large scale contribution grows with Re_τ.

Summary and conclusions

Sufficiently resolved streamwise and spanwise velocity components are obtained using a custom cross-wire probe in high Reynolds number turbulent boundary layers with Re_τ up to 10,000. The custom probe is manufactured such that the sensing elements remain parallel to the wall while the probe is inclined at 10° to the horizontal, enabling measurement as close as $z^+ \approx 10$ from the wall while also minimising the blockage effects. By changing the location of the streamwise distance from the trip and matching U_∞/ν, streamwise and spanwise velocity measurements are obtained with matched measurement volumes of approximately $14 \times 14 \times 7$ in viscous length scales across different Re_τ, isolating the effects of spatial resolution.

Resulting statistics and pre-multiplied spectra show clear scale separation in both streamwise and spanwise velocities at $Re_\tau \approx 10{,}500$. The inner site which is fixed in position and magnitude based on viscous units, represents the contribution due to the near-wall cycle. It has been suggested by Hutchins *et al.* [1] that the outer site which grows in position and magnitude when scaled with viscous units, represents the contribution due to very long meandering features or 'superstructures'. Both the streamwise and spanwise fluctuations clearly have a large scale component with a footprint that stretches to the surface. The magnitude of the large scale component appears to grow with Reynolds number. This may be related to the growth in strength of the large-scale roll-modes that have been shown to accompany superstructure events.

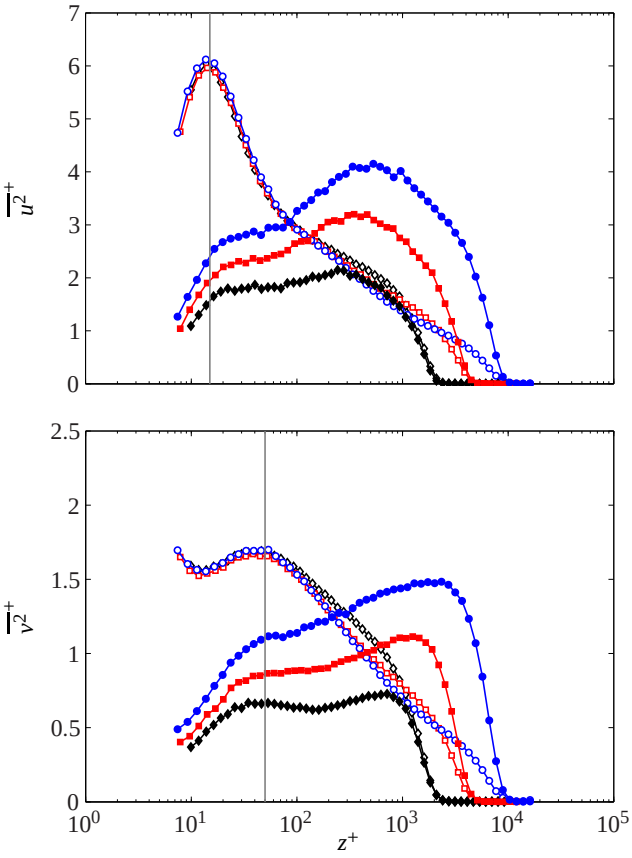

Figure 5: Contribution of the small and large scales to the turbulence intensities of streamwise (top) and spanwise (bottom) velocities; ○ - $Re_\tau \approx 10{,}500$, □ - $Re_\tau \approx 6{,}000$, ◊ - $Re_\tau \approx 3{,}000$; solid symbol - contribution from large scales; open symbol - contribution from small scales; grey lines indicate the location at $z^+ = 15$ (top) and $z^+ = 50$ (bottom).

Acknowledgements

The authors gratefully acknowledge support from the Australian Research Council.

References

[1] Hutchins, N. and Marusic, I., Evidence of very long meandering features in the logarithmic region of turbulent boundary layers, *J Fluid Mech*, **579**, 2007, 103–136.

[2] Hutchins, N., Nickels, T. B., Marusic, I. and Chong, M. S., Hot-wire spatial resolution issues in wall-bounded turbulence, *J Fluid Mech*, **635**, 2009, 103–136.

[3] Jørgensen, F. E., The computer-controlled constant-temperature anemometer: aspects of set-up, probe calibration, data acquisition and data conversion, *Exp. Fluids*, **12**, 1996, 1378–1387.

[4] Kulandaivelu, V., *Evolution of zero pressure gradient turbulent boundary layer from different initial conditions*, Ph.D. thesis, The University of Melbourne, 2012.

[5] Monkewitz, P. A., Chauhan, K. A. and Nagib, H. M., Self-consistent high-Reynolds-number asymptotics for zero-pressure-gradient turbulent boundary layers, *Phy. Fluids*, **19**, 2007, 115101.

[6] Townsend, A. A., *The structure of turbulent shear flow*, Cambridge University Press, Cambridge, UK, 1976.